Reduced tropical climate land area under global warming

Ori Adam[1], Noga Liberty-Levi[1], Michael Byrne[2], and Thomas Birner[3]

[1]Hebrew University
[2]university Saint Andrews
[3]Ludwig-Maximilians University

December 16, 2022

Abstract

Regions along the edges of the tropics host vast populations and ecosystems which are sensitive to climate change. Here we examine the extent of tropical climate land areas in the ERA5 and MERRA-2 reanalyses in high-emission scenarios of 45 models participating in phases 5 and 6 of the Coupled Model Intercomparison Project (CMIP5/6). Based on the definition of tropical climate land areas as regions where the diurnal temperature range exceeds the seasonal temperature range, we find a net reduction of tropical land area with global warming. This change is primarily due to an increased seasonal temperature range, driven by enhanced summer warming. The reduction in tropical land area is consistent with the expansion of the subtropical descending zones and with the expansion of drylands with global warming. However, the particular contributions of dynamic and thermodynamic processes are not clear.

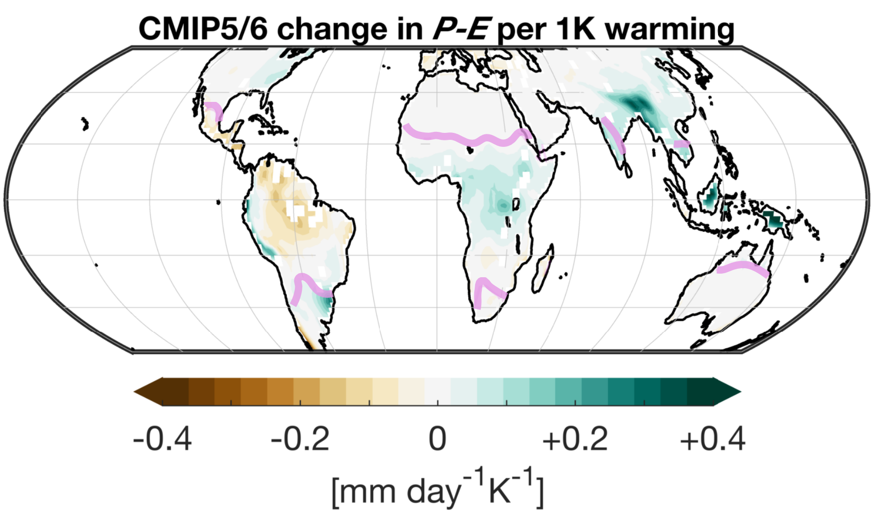

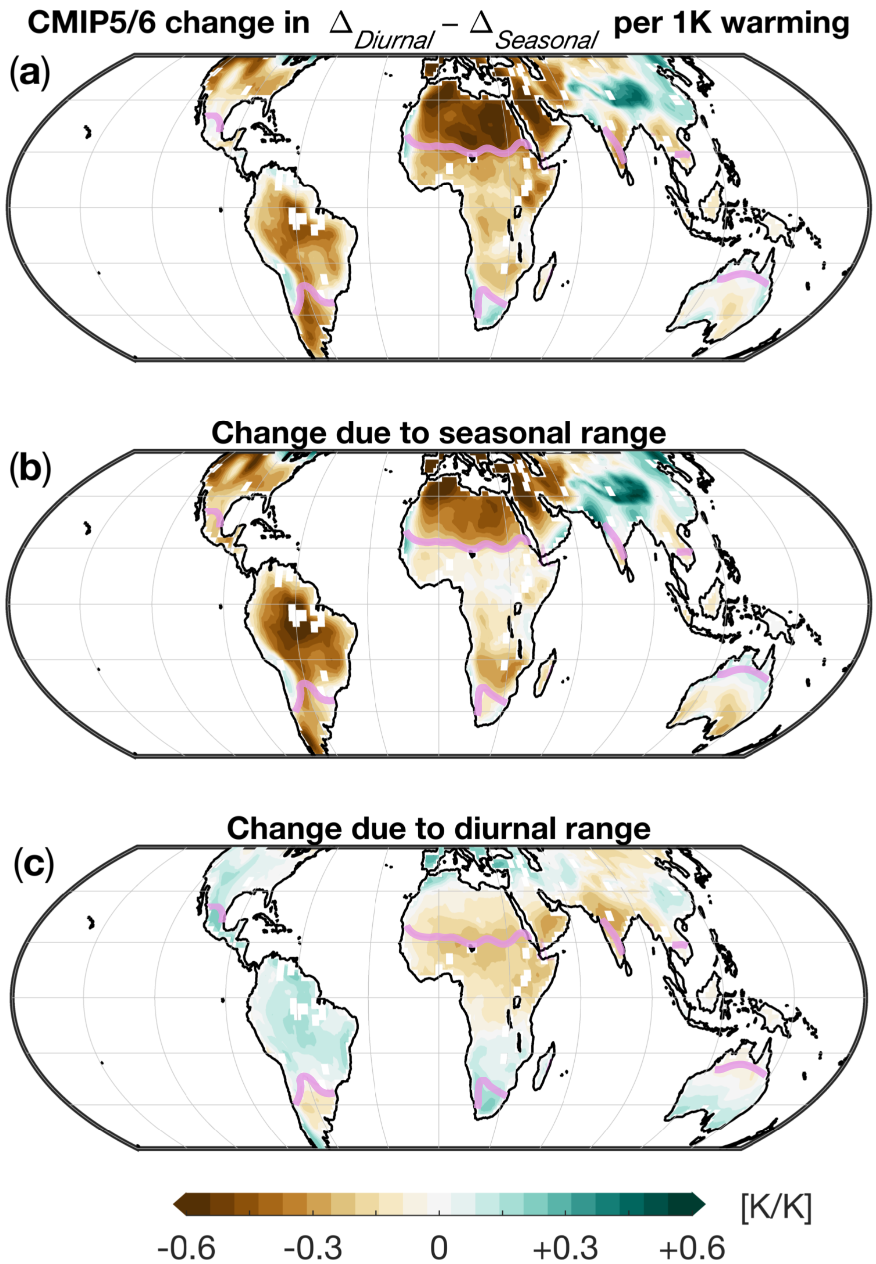
CMIP5/6 change in $\Delta_{Diurnal} - \Delta_{Seasonal}$ per 1K warming
(a)
Change due to seasonal range
(b)
Change due to diurnal range
(c)
[K/K]
-0.6
-0.3
0
+0.3
+0.6

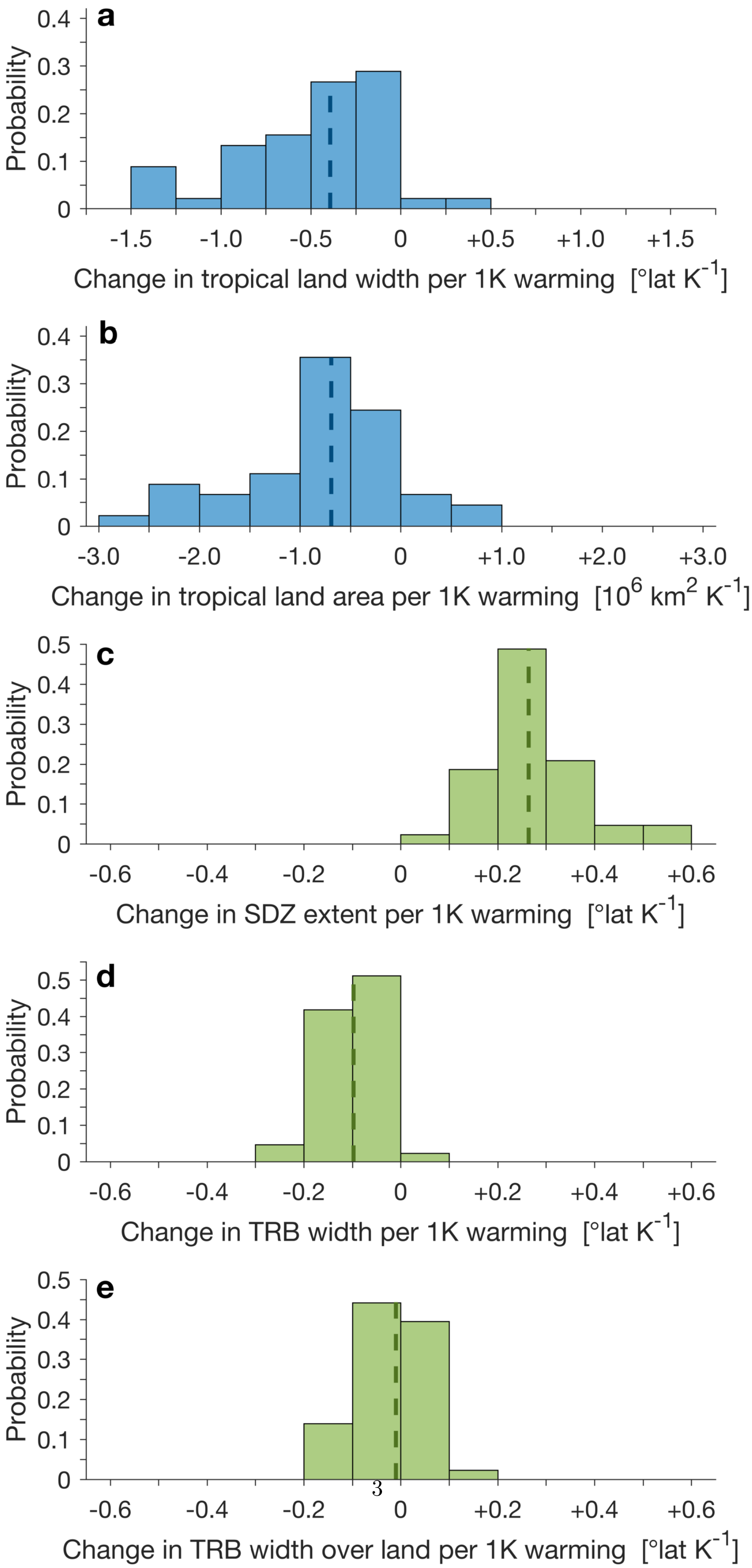
a
Probability
0.4
0.3
0.2
0.1
0
-1.5
-1.0
-0.5
0
+0.5
+1.0
+1.5
Change in tropical land width per 1K warming [°lat K-1]
b
Probability
0.4
0.3
0.2
0.1
0
-3.0
-2.0
-1.0
0
+1.0
+2.0
+3.0
Change in tropical land area per 1K warming [10^6 km^2 K-1]
c
Probability
0.5
0.4
0.3
0.2
0.1
0
-0.6
-0.4
-0.2
0
+0.2
+0.4
+0.6
Change in SDZ extent per 1K warming [°lat K-1]
d
Probability
0.5
0.4
0.3
0.2
0.1
0
-0.6
-0.4
-0.2
0
+0.2
+0.4
+0.6
Change in TRB width per 1K warming [°lat K-1]
e
Probability
0.5
0.4
0.3
0.2
0.1
0
-0.6
-0.4
-0.2
0
+0.2
+0.4
+0.6
Change in TRB width over land per 1K warming [°lat K-1]

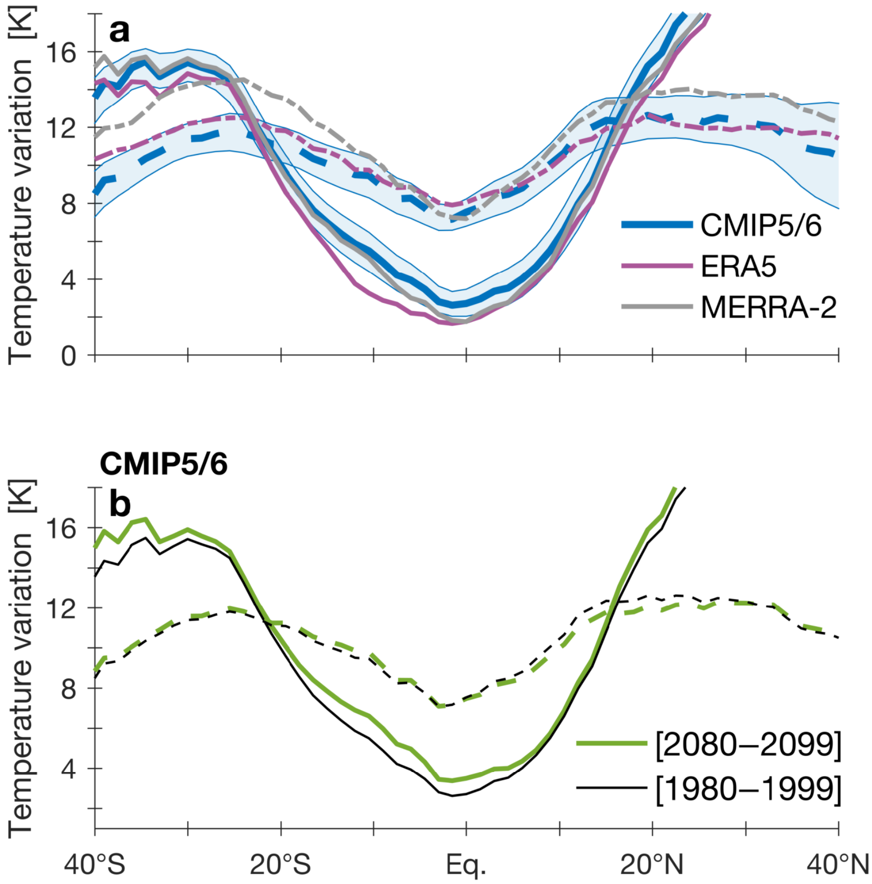
a
Temperature variation [K]
16
12
8
4
0
CMIP5/6
ERA5
MERRA-2
CMIP5/6
b
Temperature variation [K]
16
12
8
4
[2080–2099]
[1980–1999]
40°S
20°S
Eq.
20°N
40°N

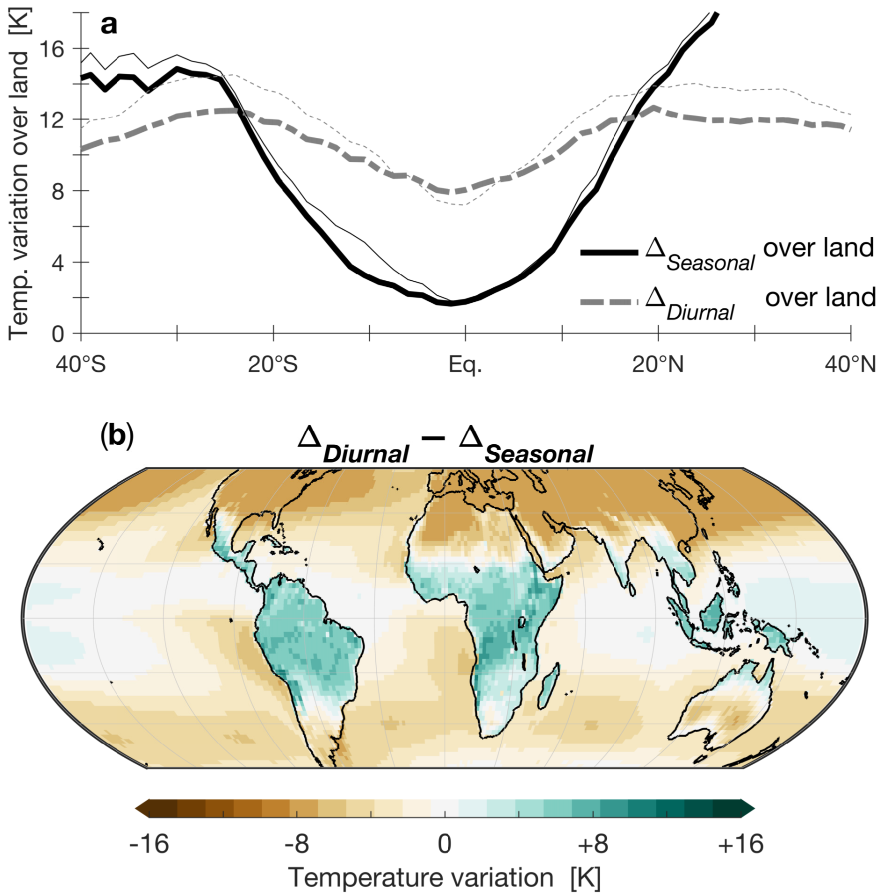
a
Temp. variation over land [K]
0
4
8
12
16
40°S
20°S
Eq.
20°N
40°N
$\Delta_{Seasonal}$ over land
$\Delta_{Diurnal}$ over land
(b)
$\Delta_{Diurnal} - \Delta_{Seasonal}$
-16
-8
0
+8
+16
Temperature variation [K]

Figure.

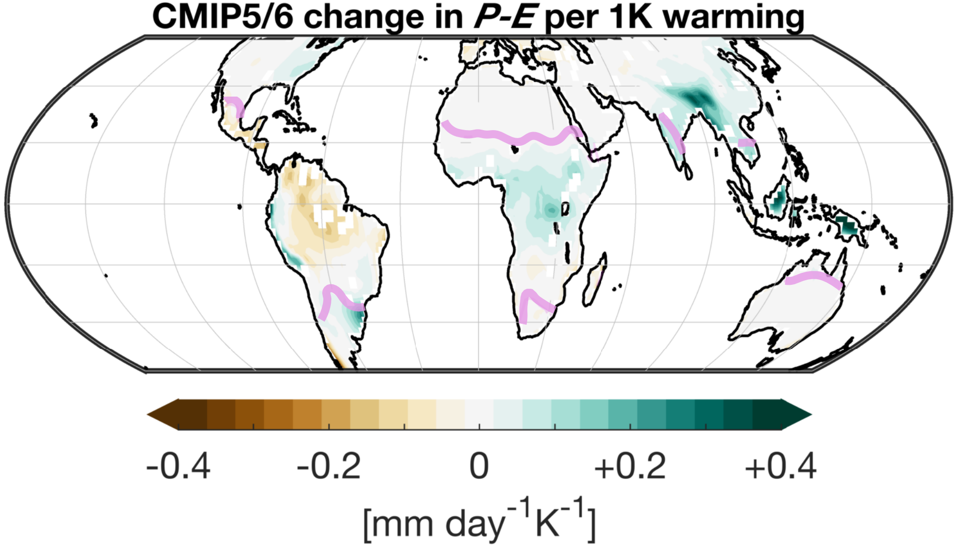

CMIP5/6 change in P-E per 1K warming
-0.4
-0.2
0
+0.2
+0.4
[mm day-1K-1]

Figure.

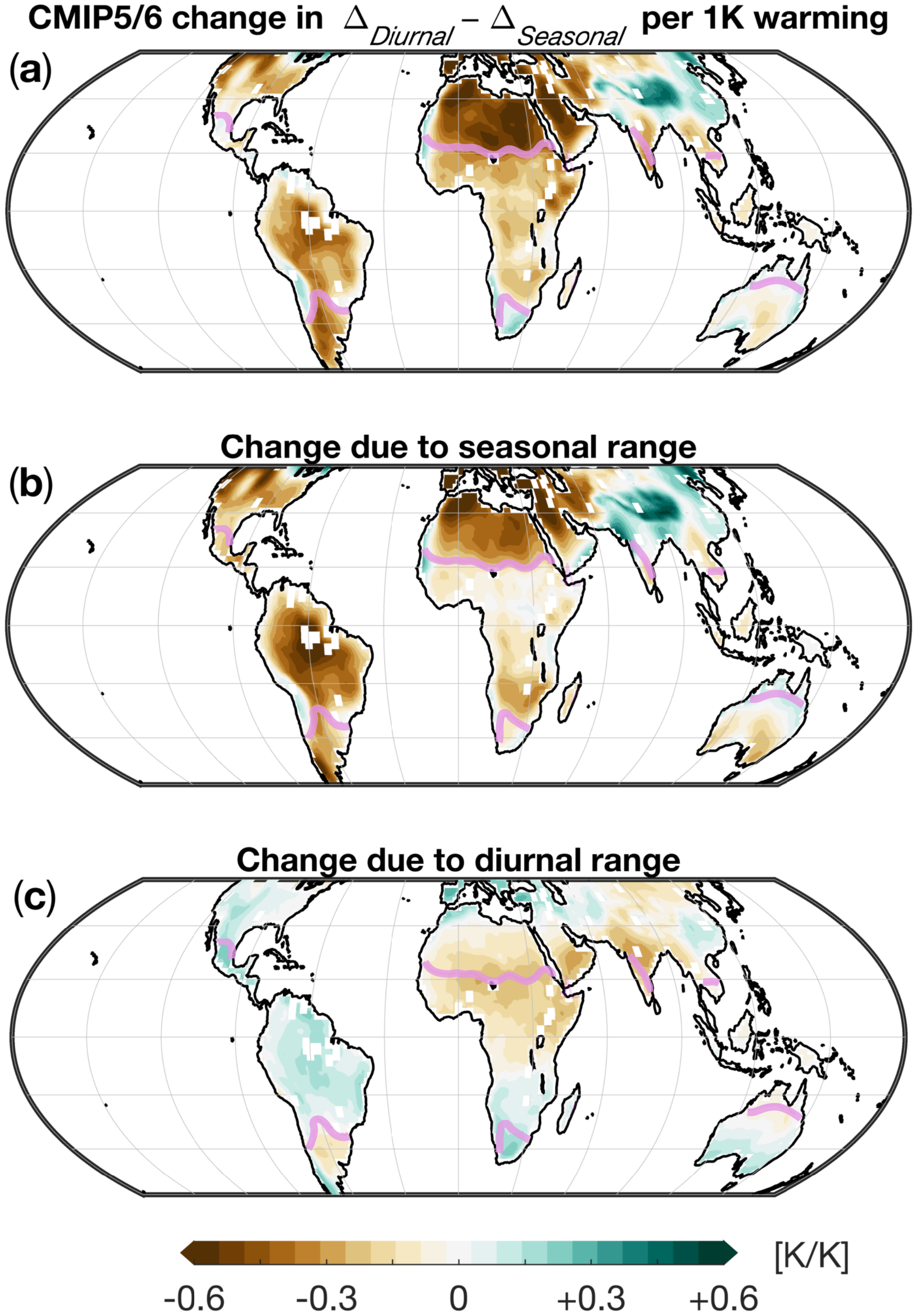

CMIP5/6 change in $\Delta_{Diurnal} - \Delta_{Seasonal}$ per 1K warming
(a)
Change due to seasonal range
(b)
Change due to diurnal range
(c)
[K/K]
-0.6
-0.3
0
+0.3
+0.6

Figure.

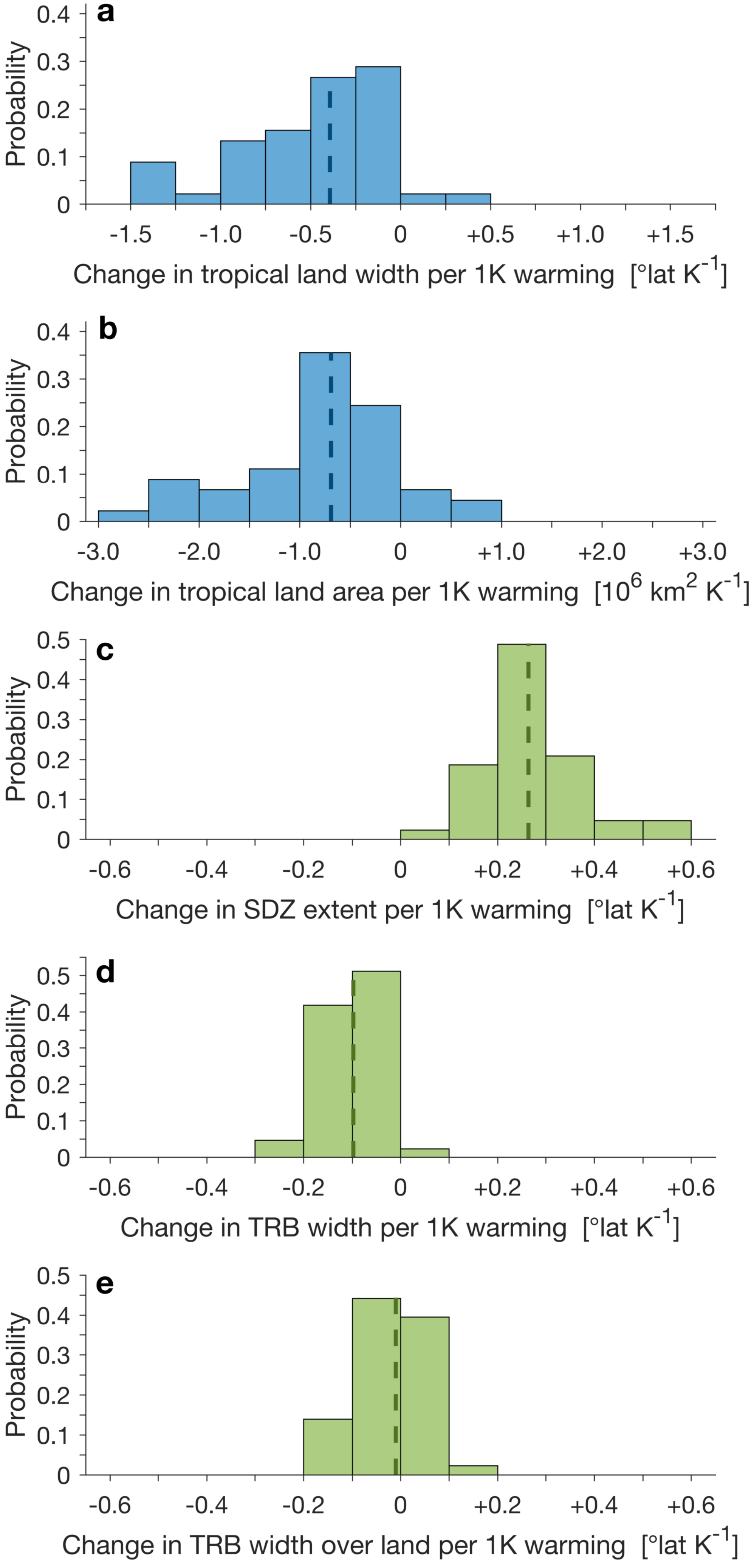
a
Probability
0
0.1
0.2
0.3
0.4
-1.5
-1.0
-0.5
0
+0.5
+1.0
+1.5
Change in tropical land width per 1K warming [°lat K^-1]
b
Probability
0
0.1
0.2
0.3
0.4
-3.0
-2.0
-1.0
0
+1.0
+2.0
+3.0
Change in tropical land area per 1K warming [10^6 km^2 K^-1]
c
Probability
0
0.1
0.2
0.3
0.4
0.5
-0.6
-0.4
-0.2
0
+0.2
+0.4
+0.6
Change in SDZ extent per 1K warming [°lat K^-1]
d
Probability
0
0.1
0.2
0.3
0.4
0.5
-0.6
-0.4
-0.2
0
+0.2
+0.4
+0.6
Change in TRB width per 1K warming [°lat K^-1]
e
Probability
0
0.1
0.2
0.3
0.4
0.5
-0.6
-0.4
-0.2
0
+0.2
+0.4
+0.6
Change in TRB width over land per 1K warming [°lat K^-1]

Figure.

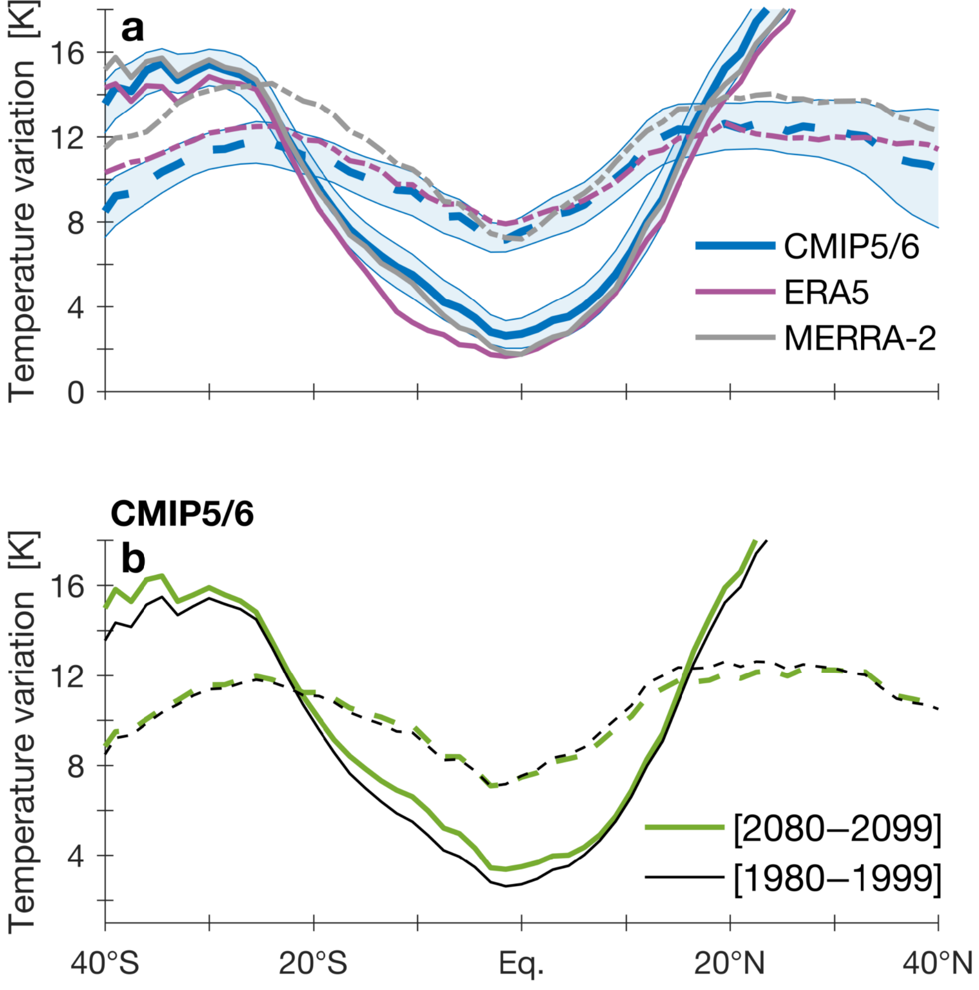

a
Temperature variation [K]
16
12
8
4
0
CMIP5/6
ERA5
MERRA-2
CMIP5/6
b
Temperature variation [K]
16
12
8
4
[2080–2099]
[1980–1999]
40°S
20°S
Eq.
20°N
40°N

Figure.

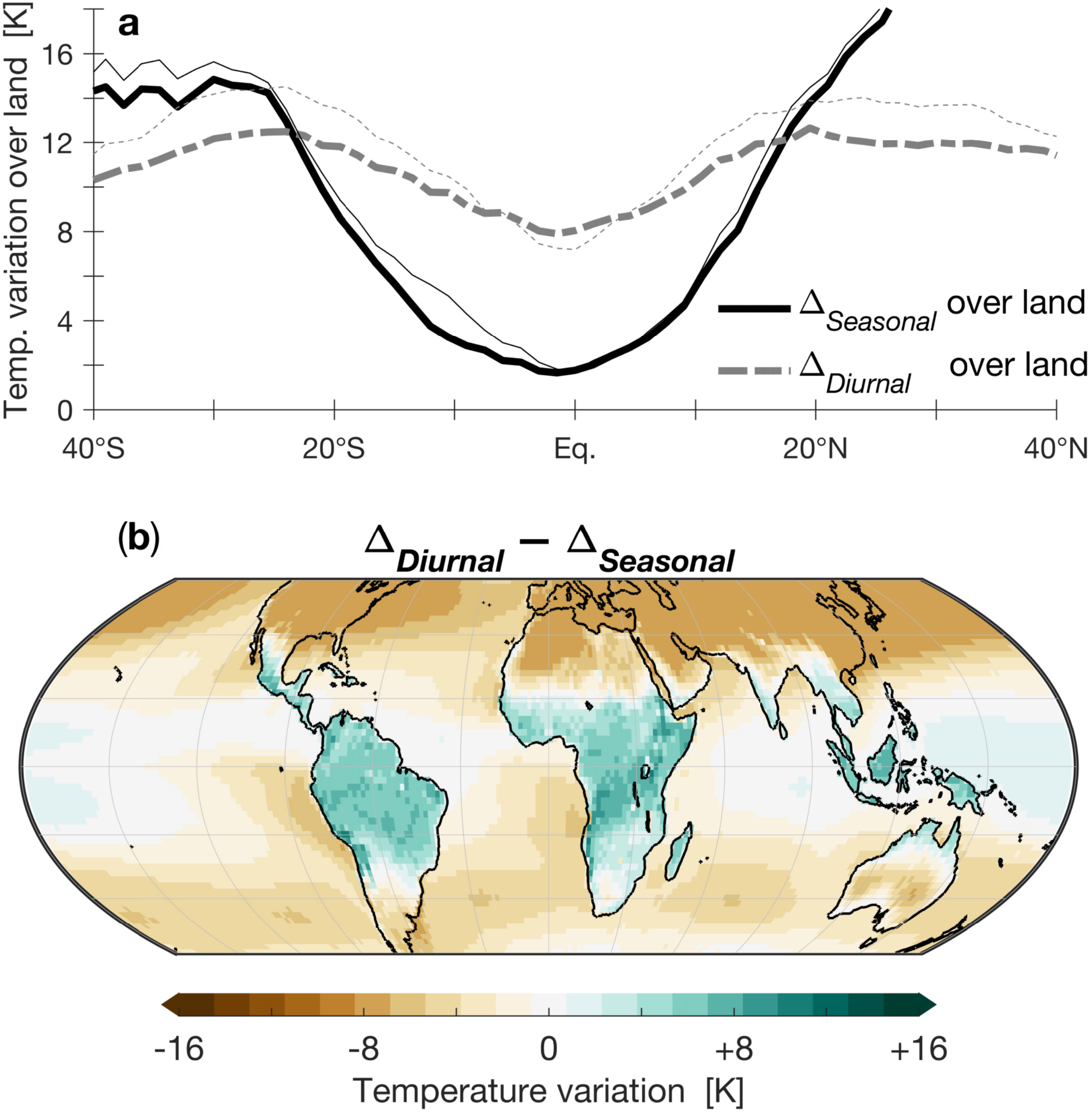

a
Temp. variation over land [K]
0
4
8
12
16
40°S
20°S
Eq.
20°N
40°N
$\Delta_{Seasonal}$ over land
$\Delta_{Diurnal}$ over land
(b)
$\Delta_{Diurnal} - \Delta_{Seasonal}$
-16
-8
0
+8
+16
Temperature variation [K]

Reduced tropical climate land area under global warming

Ori Adam[1], Noga Liberty-Levi[1], Michael Byrne[2,3], Thomas Birner[4]

[1]The Fredy and Nadine Herrmann Institute of Earth Sciences, The Hebrew University, Jerusalem, Israel
[2]School of Earth and Environmental Sciences, University of St Andrews, St Andrews, UK
[3]Department of Physics, University of Oxford, Oxford, UK
[4]Meteorologisches Institut, Ludwig-Maximilians-Universität, Munich, Germany

Key Points:

- Net tropical climate land area, defined by smaller seasonal than diurnal temperature range, is projected to decrease in a warming climate
- The decrease is primarily due to enhanced summer warming, leading to elevated seasonal temperature range in the tropics
- Changes are consistent with but not clearly related to the expansion of the subtropical dry zones with global warming

Corresponding author: Ori Adam, `ori.adam@mail.huji.ac.il`

Abstract

Regions along the edges of the tropics host vast populations and ecosystems which are sensitive to climate change. Here we examine the extent of tropical climate land areas in the ERA5 and MERRA-2 reanalyses in high-emission scenarios of 45 models participating in phases 5 and 6 of the Coupled Model Intercomparison Project (CMIP5/6). Based on the definition of tropical climate land areas as regions where the diurnal temperature range exceeds the seasonal temperature range, we find a net reduction of tropical land area with global warming. This change is primarily due to an increased seasonal temperature range, driven by enhanced summer warming. The reduction in tropical land area is consistent with the expansion of the subtropical descending zones and with the expansion of drylands with global warming. However, the particular contributions of dynamic and thermodynamic processes are not clear.

Plain Language Summary

Tropical climate land areas host about 40% of the world's population and 80% of the world's biodiversity. Changes in the extent of tropical climate land areas, which generally border semi-arid climate zones, can therefore carry vast ecological and socio-economic implications. Tropical climate land areas are generally defined as regions where the daily temperature range exceeds the seasonal temperature range. Based on this definition we find a net decrease in tropical land area in climate model projections of greenhouse-gas-induced global warming. The net reduction in tropical land area is driven primarily by increased seasonal temperature range, due to enhanced summer warming. The reduction in tropical land area is consistent with the expansion of the subtropical descending zones and with the expansion of drylands with global warming. However, the specific contributions of dynamic and hydrological processes are not clear.

1 Introduction

Tropical climate land areas host about 40% of the world's population and 80% of the world's biodiversity. Changes in the extent of tropical climate land areas, which generally border semi-arid climate zones, can therefore carry vast ecological and socio-economic implications (Ruane et al., 2021; Grünzweig et al., 2022). It is now well established that the tropical overturning circulation in the atmosphere has widened meridionally in recent decades, pushing subtropical dry zones poleward (Lu et al., 2007; Seidel et al., 2008), a tendency expected to continue under global warming (for reviews, see Staten et al., 2018, 2020). The extent of global drylands is similarly observed and projected to increase with global warming, partly at the expense of tropical land areas, due to increased global aridity (Feng & Fu, 2013; Huang et al., 2017). However, regional trends and the dynamic and thermodynamic drivers that underlie regional variations in the extent of the tropics remain poorly understood (Bony et al., 2015; Nguyen et al., 2018; Grise et al., 2018; Staten et al., 2019; Palmer & Stevens, 2019; D'Agostino et al., 2020). Here we analyze projected changes in the extent of tropical climate land areas using a simple definition of tropical zones based on temperature variations, and relate these changes to the expansion of the subtropical dry zones.

In the present climate, seasonal temperature variations nearly vanish near the equator and generally increase toward the poles – in accordance with seasonal insolation (Riehl et al., 1979). Diurnal temperature variations are similarly lower near the equator but vary modestly between tropical and subtropical latitudes (Riehl et al., 1979; Yang & Slingo, 2001). In addition, owing to the large contrast in heat capacity, tropical surface temperature variations over land are significantly larger than over ocean. Specifically, land variations are larger by a factor of about 10 on diurnal timescales, and by a factor of about 2 on seasonal timescales, making diurnal surface temperatures variations significantly larger than seasonal variations in the tropics (Riehl, 1954; Riehl et al., 1979). Tropical

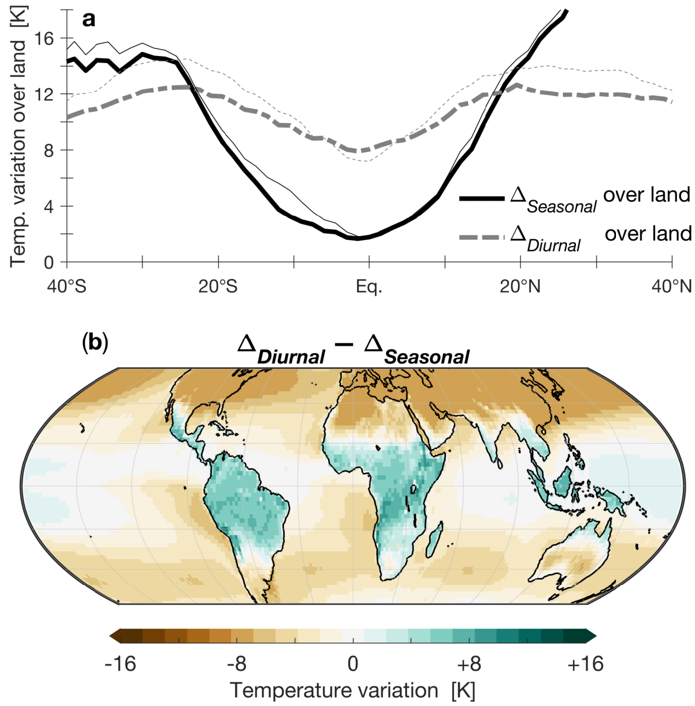

Figure 1. (**a**) Seasonal (solid black) and diurnal (dashed gray) surface temperature ranges ($\Delta_{Seasonal}$ and $\Delta_{Diurnal}$, respectively), zonally averaged over land areas. (**b**) Global $\Delta_{Diurnal} - \Delta_{Seasonal}$. Data shown for climatological values of the European Centre for Medium-Range Weather Forecasts ERA5 dataset (panel b and thick lines in panel a, Hersbach et al., 2020), and for the National Aeronautics and Space Administration MERRA-2 dataset (thin lines in panel a, Gelaro et al., 2017), for the years 1980–2020. See section 2 for details on the data and calculations.

climate land areas are therefore conveniently defined as land regions where the diurnal temperature range exceeds the seasonal temperature range – a definition commonly attributed to Riehl et al. (1979), but first proposed by Troll (1943) and demonstrated in Paffen (1967).

Figure 1 shows the observed climatological mean differences over land between maximal and minimal diurnal surface air temperatures ($\Delta_{Diurnal}$) and between the hottest and coldest months in each year ($\Delta_{Seasonal}$). Tropical climate land areas, where $\Delta_{Diurnal} > \Delta_{Seasonal}$, are clearly delineated from subtropical areas, with mean edges at about 24°S and 17°N. Changes associated with global warming in the extent of tropical land areas, as defined above, thus depend on the responses of seasonal and diurnal surface temperature variations.

The sensitivities of seasonal and diurnal temperature variability to global warming have been extensively analyzed in modeling and observational studies (e.g., Stouffer & Wetherald, 2007; Manabe et al., 2011; Sobel & Camargo, 2011; Dwyer et al., 2012; Stine & Huybers, 2012; Donohoe & Battisti, 2013; Holmes et al., 2016; Yettella & England, 2018; Chen et al., 2019). In high latitudes, the seasonal temperature range generally decreases with global warming due to enhanced winter warming (e.g., Manabe et al., 2011; Dwyer et al., 2012; Chen et al., 2019). The diurnal temperature range has likewise generally decreased globally over the past century, especially in higher latitudes, due to enhanced nighttime warming (Wild, 2009; Thorne, Menne, et al., 2016; Thorne, Donat, et al., 2016; K. Wang & Clow, 2020).

In contrast, at low latitudes global warming is associated with a weak general increase in both seasonal and diurnal surface temperature variability. The increase in the seasonal temperature range is mainly attributed to reduced evaporative cooling during summer, caused by decreased relative humidity and weakened circulation (Sobel & Camargo, 2011; Chen et al., 2019). The diurnal temperature range is generally lower during summer, and therefore affected by the elevated summer temperatures (Yang & Slingo, 2001; Geerts, 2003). However, both seasonal and diurnal temperature variations over land depend strongly on local processes which are typically not well simulated by climate models. There is therefore generally poor consistency across climate models and between observed and projected changes in both seasonal and diurnal tropical temperature variations, especially on regional scales (Dwyer et al., 2012; C. Wang et al., 2014; Thorne, Donat, et al., 2016; Yin & Porporato, 2017; Chen et al., 2019; K. Wang & Clow, 2020).

Here we use the temperature-range definition of tropical climate land areas to examine the extent of tropical land areas in reanalyses and in projections by coupled climate models. Our methodology is described in Section 2, followed by our results and a discussion in Sections 3 and 4.

2 Data and methods

Observationally constrained data is taken from the European Center for Medium-Range Weather Forecasts (ECMWF) ERA5 reanalysis (0.25° X 0.25°resolution; Hersbach et al., 2020), and from the National Aeronautics and Space Administration MERRA-2 reanalysis (0.625° X 0.5°; Gelaro et al., 2017) for the years 1980–2020.

The seasonal temperature range ($\Delta_{Seasonal}$) is calculated as the difference between the months with hottest and coldest surface air temperatures (2m) in each year at each grid point. The diurnal temperature range ($\Delta_{Diurnal}$) is calculated as the annual mean difference between monthly maximal and minimal diurnal surface temperatures at each grid point, derived from hourly data. We derive two parameters from the difference between $\Delta_{Diurnal}$ and $\Delta_{Seasonal}$: (i) Tropical land width is calculated as the distance between the northern and southern latitudes where $\Delta_{Diurnal} - \Delta_{Seasonal}$ changes sign; (ii) Tropical land area is calculated as the area-weighted sum over all land grid points in which $\Delta_{Diurnal} > \Delta_{Seasonal}$ (lakes are excluded). For reference, the climatologies of observed seasonal and diurnal surface temperature ranges are shown and discussed in the Supporting Information (Figure S1).

We also analyze tropical temperature variations in 27 climate models from phase 5 (Taylor et al., 2012) and 18 models from phase 6 (Eyring et al., 2016) of the Coupled Model Intercomparison Project (CMIP5/6), based on availability (Table S1). For CMIP5/6 models, $\Delta_{Seasonal}$ is calculated from monthly surface air temperature fields (i.e., the 'tas' variable), and $\Delta_{Diurnal}$ is calculated as the annual mean difference between monthly maximal and minimal daily surface temperatures at each grid point (i.e., using the 'tasmax' and 'tasmin' variables). For each model we use data only from the first realization (ensemble members 'r1i1p1' and 'r1i1p1f1' for CMIP5 and CMIP6, respectively), linearly interpolated to a common 1.5°×1.5° horizontal grid.

To examine the relation of tropical land areas to the subtropical dry zones, we analyze variations in precipitation minus evaporation ($P - E$) in the 27 CMIP5 models and in 16 of the 18 CMIP6 models ($P-E$ data is not available for the 'GFDL-ESM4' and 'CAS-ESM2-0' models; see Table S1). Specifically, the poleward extent of the subtropical dry zones increases with global warming, and is known to strongly covary with the width of the tropical meridional overturning circulation (Lu et al., 2007; Seviour et al., 2018). We calculate the poleward extent of the subtropical dry zones as the subtropical latitudes where the zonal mean $P-E$ (over land and ocean) changes sign, averaged over the northern and southern hemispheres, using the TropD software package (Adam et al., 2018). (Note that this definition cannot be applied to only land areas, because evaporation nearly vanishes over land.) We also analyze the width of the tropical rain belt (or the width of the intertropical convergence zone), which is projected to decrease under global warming (Byrne & Schneider, 2016b). We estimate the width of the tropical rain belt (TRB) as the standard deviation of the meridional distribution of precipitation equatorward of 20°, which is well correlated with other indices of the TRB width (Adam et al., 2022, see the Appendix for details). We apply this definition to the zonal mean precipitation (over land and ocean), as well as to precipitation zonally averaged over land.

To gauge model biases, we compare historical simulations averaged over the period 1980–1999 with the ERA5 and MERRA-2 reanalyses. For assessing the sensitivity to global warming, we take the averaged difference between years 2080–2099 in the RCP85 (CMIP5) and SSP585 (CMIP6) scenarios, in which pre-industrial CO_2 levels are quadrupled by the end of the 21st century, and the historical simulations. As shown in Figure S2, the zonally land-averaged representation of $\Delta_{Seasonal}$ and $\Delta_{Diurnal}$ in the two CMIP phases is statistically indistinguishable; we therefore analyze the two phases jointly. We note that CMIP5/6 models are known to have regional biases in seasonal temperature variability, mainly associated with coupled large-scale circulation (C. Wang et al., 2014; Chen et al., 2019), as well as deficiencies in the representation of diurnal temperature variations, associated with biases in cloud, surface, and vegetation processes (Yin & Porporato, 2017; K. Wang & Clow, 2020).

3 Results

3.1 Zonal mean trends

Figure 2a compares $\Delta_{Seasonal}$ and $\Delta_{Diurnal}$ in the CMIP5/6 historical simulations and in the ERA5 and MERRA-2 datasets, zonally averaged over land. In the subtropical latitudes where $\Delta_{Diuranl}-\Delta_{Seasonal}$ changes sign, the model seasonal temperature ranges are in broad agreement with the reanalyses. However, diurnal temperature ranges do not agree across both models and reanalyses, for example in the southern hemisphere where the models underestimate $\Delta_{Diurnal}$ (more so when compared with MERRA-2), reflecting the large uncertainty in simulating diurnal temperature variations (K. Wang & Clow, 2020). We therefore proceed with the analysis while acknowledging the large uncertainties associated with changes in diurnal temperature variations. In addition, given the discrepancies across reanalyses and the significant role of natural variability in observed tropical widening trends (Nguyen et al., 2013; Adam et al., 2014; Staten et al., 2018), our analysis hereon focuses only on long-term trends associated with global warming in CMIP5/6 projections.

Figure 2b shows the CMIP5/6 ensemble means of $\Delta_{Seasonal}$ and $\Delta_{Diurnal}$, zonally averaged over land, in historical simulations and in projections. The projected changes show: (i) generally increased tropical $\Delta_{Seasonal}$, and (ii) reduced $\Delta_{Diurnal}$ in the northern hemisphere and increased $\Delta_{Diurnal}$ in the southern hemisphere, suggesting an overall decrease in the extent of tropical land area. Consistent with previous analyses, since $\Delta_{Seasonal}$ increases with mean temperature, the projected increase in $\Delta_{Seasonal}$ is caused by enhanced warming during the warm season (e.g., Chen et al., 2019).

Figure 3a,b shows model probability distribution functions (PDFs) of the projected changes per 1K global warming of tropical land width (mean latitudinal extent of land where $\Delta_{Diurnal} > \Delta_{Seasonal}$) and of tropical land area (net land area where $\Delta_{Diurnal} > \Delta_{Seasonal}$). A shift toward reduced tropical width and area is seen in nearly all of the models, indicating a reduced net tropical extent under global warming (ensemble mean

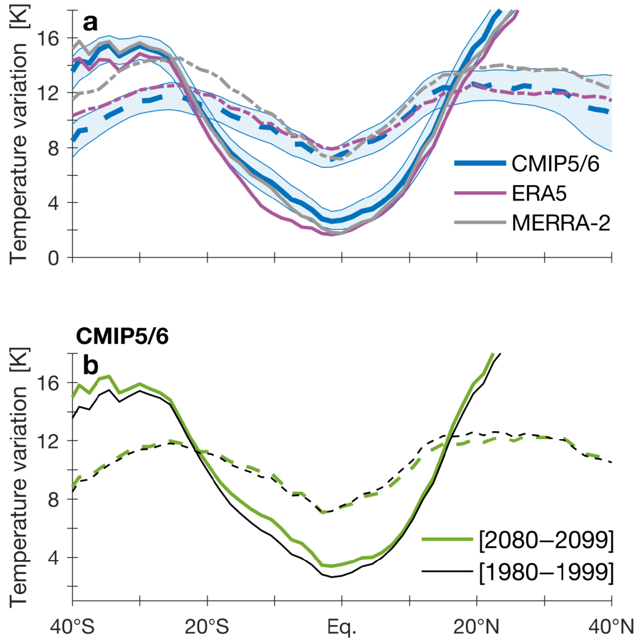

Figure 2. (**a**) Amplitudes of seasonal ($\Delta_{Seasonal}$, solid) and diurnal ($\Delta_{Diurnal}$, dashed) surface temperature ranges, zonally averaged over land, for CMIP5/6 historical simulations (blue) and for the ERA5 (purple) and MERRA-2 (gray) reanalyses. Shading indicates ±1 standard deviation across models. (**b**) Ensemble mean CMIP5/6 values of $\Delta_{Diurnal}$ and $\Delta_{Seasonal}$, zonally averaged over land, for the periods 1980–1999 (black, historical simulations) and 2080–2099 (green, RCP85/SSP585 simulations).

decrease in width and area per 1K is 0.48° and $0.78{\cdot}10^6$ km^2; see Figure S3 for the corresponding end of 20th and end of 21st centuries' PDFs).

Figure 3c,d shows the projected changes in the poleward extent of the subtropical dry zones (SDZs) and in the width of the tropical rain belt (TRB), zonally averaged over land and ocean. A clear poleward expansion of the SDZs is seen, associated with a widening of the tropical meridional overturning circulation (, e.g., Seviour et al., 2018; Waugh et al., 2018), and a narrowing of the TRB, associated with increased energy transport out of the rising branch of the tropical overturning circulation (Byrne & Schneider, 2016a). These changes indicate an expansion of the SDZs on both their poleward and equatorward edges (Byrne & Schneider, 2016a). However, as shown in Figure 3e, there is no statistically significant change in the width of the TRB over land. The narrowing of tropical climate land area is therefore not clearly related to the expansion of the subtropical descending zones, which is attributed to changes in the tropical meridional overturning circulation, but is manifested primarily over ocean due to confounding effects by land-ocean temperature contrast and radiative forcing (He & Soden, 2017).

3.2 Regional trends

We now turn to examine regional changes. Given the similarities between the width and area indices, and given that tropical zonally-varying width is not well defined in narrow continent strips (Figure 1b), we focus our regional analysis on tropical land area.

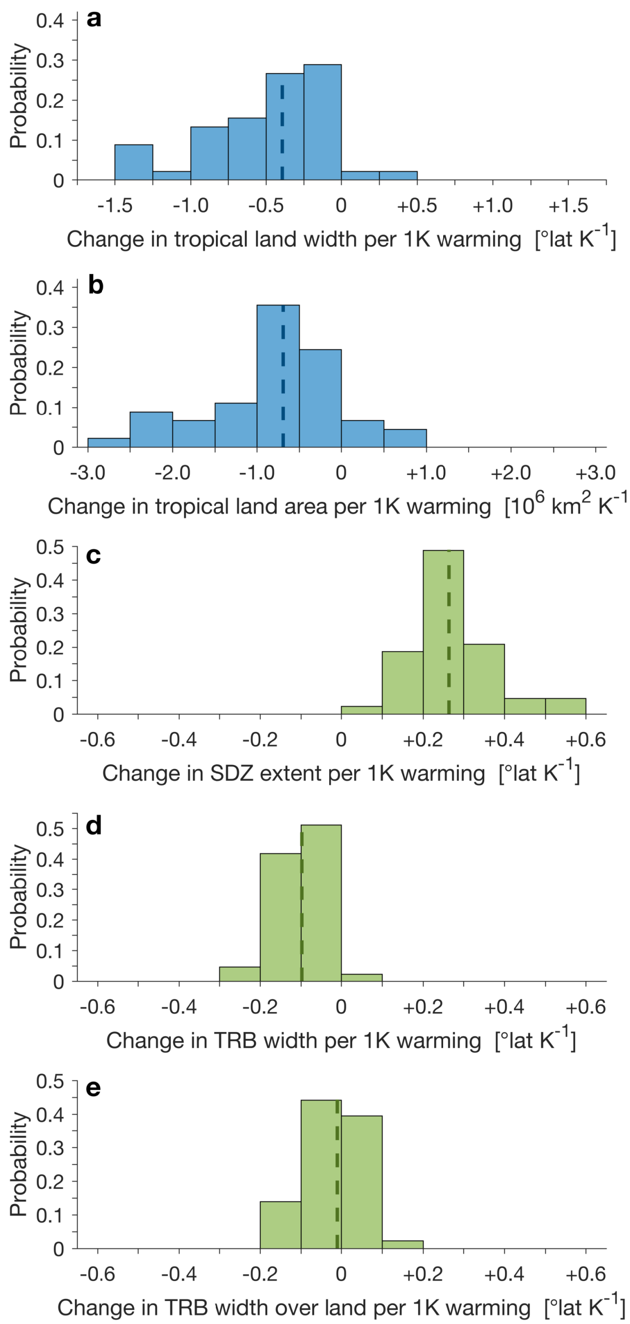

Figure 3. Probability distribution functions of changes per 1K global mean temperature warming in (**a**) tropical land width (mean latitudinal extent of land where $\Delta_{Diurnal} > \Delta_{Seasonal}$), (**b**) tropical land area (net land area where $\Delta_{Diurnal} > \Delta_{Seasonal}$), (**c**) extent of the zonal mean (over land and ocean) subtropical dry zones (SDZs), (**d**) width of the zonal mean tropical rain belt (TRB), and (**e**) width of the TRB averaged over land. Vertical lines show medians. The PDFs are composed of 45 models in panels a and b, and of 43 models in panels c–e.

Figure 4a shows the projected ensemble-mean changes per 1K warming in $\Delta_{Diurnal} - \Delta_{Seasonal}$. Significant reduction of tropical land area is seen over Africa and the Americas, and to a lesser degree over the Asian and western Pacific sectors (see Figures S4

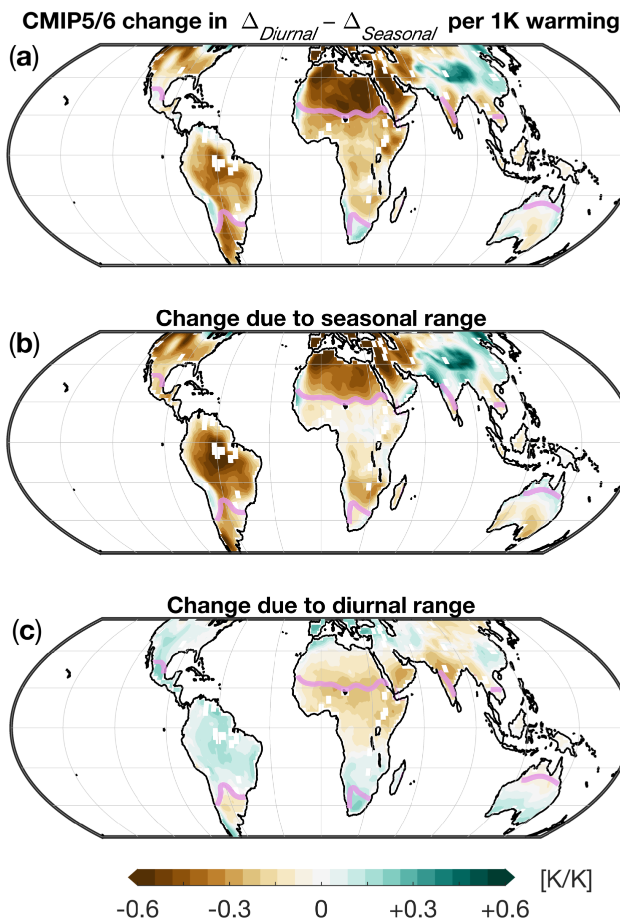

Figure 4. Change in $\Delta_{Diurnal} - \Delta_{Seasonal}$ in the CMIP5/6 ensemble mean per 1K global mean temperature warming. (**a**) total change; (**b**) change due to $\Delta_{Seasonal}$ (i.e., $\Delta_{Diurnal}$ is held fixed); (**c**) change due to $\Delta_{Diurnal}$ (i.e., $\Delta_{Seasonal}$ is held fixed). Pink lines show latitudes where $\Delta_{Diurnal} - \Delta_{Seasonal} = 0$.

and S5 for PDFs of the regional changes). Specifically, the ensemble-mean projected regional changes in tropical land area per 1K are -0.31·10^6 km^2 over Africa, -0.43·10^6 km^2 over the Americas, and -0.03·10^6 km^2 over Asia and the western Pacific sectors.

The specific contributions of changes in $\Delta_{Seasonal}$ and $\Delta_{Diurnal}$ are shown in Figure 4b,c. Most of the reduction in net tropical land area is due to increased $\Delta_{Seasonal}$, with $\Delta_{Diurnal}$ having a generally small reinforcing effect over northern Africa, and a balancing effect elsewhere. Therefore, despite the large uncertainties in projected changes in the diurnal temperature range, the reduction of tropical land area is a robust response to global warming, associated primarily with increased seasonal temperature range in the tropics.

Since the increased seasonal temperature range is associated with reduced evaporative cooling during summer (Sobel & Camargo, 2011; Chen et al., 2019), we examine the ensemble-mean changes in precipitation minus evaporation ($P-E$), normalized per 1K global warming, in Figure 5. Drying is consistent with increased seasonal temperature range over northern America and southern Africa. But it is likely not a key driver of the increased temperature range in the already-dry northern Africa, and in the wet-

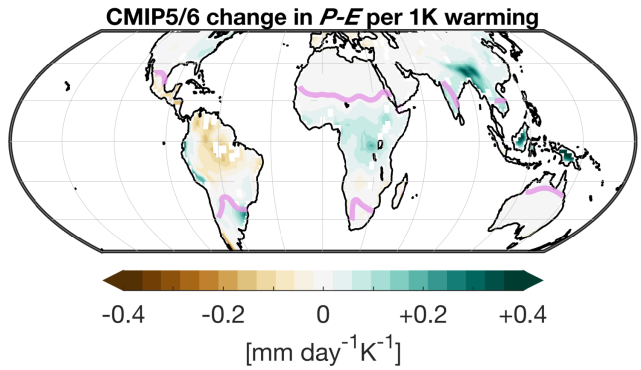

Figure 5. CMIP5/6 ensemble mean projected changes in precipitation minus evaporation ($P - E$) over land per 1K warming. Pink lines show latitudes where $\Delta_{Diurnal} - \Delta_{Seasonal} = 0$.

ter southern America and parts of the Asian sector. Thus, the decreased extent of tropical land areas, as defined here, cannot be generally attributed to drying.

4 Discussion

Tropical climate land areas can be defined as regions where the diurnal surface temperature range exceeds the seasonal surface temperature range (Figure 1). Based on this definition we find a robust reduction of tropical land area with global warming in a cohort of 27 CMIP5 and 18 CMIP6 models forced with high-emission scenarios.

The projected decrease in tropical land area is driven primarily by an increased seasonal temperature range (Figure 2b), consistently seen across regions (Fig. 4b), caused by enhanced summer warming (Sobel & Camargo, 2011; Chen et al., 2019). The diurnal temperature range generally decreases in the northern hemisphere and increases in the southern hemisphere (Figure 2b), and has an overall small contribution to the changes in tropical land area (Figure 4c). Thus, despite large uncertainties in simulated trends of the diurnal temperature range, the reduction of tropical land area with global warming is a robust response, seen in nearly all of the CMIP5/6 models (Figure 3a,b).

The net loss of tropical land area with global warming coincides with the projected expansion of the subtropical descending zones on both their equatorward and poleward edges (Lu et al., 2007; Lau & Kim, 2015), associated with dynamic processes, and with the projected global expansion of drylands, due to increased aridity (Huang et al., 2017). However, the reduction in tropical land area is not clearly related to either of these dynamic and thermodynamic trends. Specifically, the expansion of the subtropical descending zones is caused by the widening of the mean meridional overturning circulation (MOC), which is also observed across regions (Grise et al., 2018; Staten et al., 2019; D'Agostino et al., 2020), and the narrowing of the width of the tropical rain belt (i.e., the rising branch of the MOC Byrne & Schneider, 2016b; Byrne et al., 2018; Donohoe et al., 2019). But the width of the tropical rain belt does not decrease over land, and is therefore not clearly related to changes in the MOC (Figure 3). Similarly, changes in the seasonal and diurnal temperature ranges are not directly related to changes in precipitation minus evaporation (Figure 5). Moreover, in the subtropics, where tropical climate land area is lost, CMIP5 models project transitions of land areas from both wet-to-drier and from dry-to-wetter conditions (Figure 5; Feng & Fu, 2013; Grünzweig et al., 2022). Therefore, dynamic and thermodynamic drivers likely have diverse effects on the reduction in tropical climate land area. Further analysis is required to to better understand the causes and implications of reduced tropical land area, especially on regional to local scales.

Appendix A Width of the tropical rain belt

Defining the centroid latitude of the meridional distribution of zonal-mean precipitation P as

$$\phi_{cent} = \int_{20^\circ S}^{20^\circ N} P(\phi)\phi\cos(\phi)\mathrm{d}\phi, \tag{A1}$$

the width of the tropical rain belt (TRB) is estimated as the standard deviation of the meridional distribution of precipitation,

$$\mathrm{W}_{TRB} = \left[\frac{\int_{20^\circ S}^{20^\circ N} P(\phi)(\phi - \phi_{cent})^2\cos(\phi)\mathrm{d}\phi}{\int_{20^\circ S}^{20^\circ N} P(\phi)\cos(\phi)\mathrm{d}\phi}\right]^{\frac{1}{2}}. \tag{A2}$$

This width estimate is generally correlated with other TRB width indices across CMIP5/6 models (Adam et al., 2022), and can be consistently applied to global and over-land zonal averages of precipitation. Results based on this estimate are also not statistically different from those obtained using TRB width defined as the difference between the northern and southern hemisphere precipitation centroids, used by Donohoe et al. (2019). Other indices of of TRB width which rely on the meridional mass streamfunction or geometric quantities of the precipitation distribution (Popp & Lutsko, 2017; Byrne et al., 2018) cannot be applied over land due to the regional and irregular precipitation distributions.

Data availability statement

All of the data used in the analyses presented here is publicly available. We thank the climate modeling groups for producing and making available their model output, the Earth System Grid Federation (ESGF) for archiving the data and providing access, and the multiple funding agencies who support CMIP and ESGF. All CMIP data analyzed here are available from the ESGF at https://esgf-node.llnl.gov/projects/esgf-llnl. The CMIP5 and CMIP6 models used can be found in Table S1

Acknowledgments

OA acknowledges support by ISF grant 1022/21.

References

Adam, O., Farnsworth, A., & Lunt, D. J. (2022). Modality of the tropical rain belt across models and simulated climates. *Journal of Climate*(10.1175/JCLI-D-22-0521.1), –.

Adam, O., Grise, K. M., Staten, P., Simpson, I. R., Davis, S. M., Davis, N. A., ... Ming, A. (2018). The TropD software package (v1): standardized methods for calculating tropical-width diagnostics. *Geosci. Model Dev.*, *11*, 4339-4357. doi: 10.5194/gmd-11-4339-2018

Adam, O., Schneider, T., & Harnik, N. (2014). Role of changes in mean temperatures versus temperature gradients in the recent widening of the Hadley circulation. *J. Climate*, *27*, 7450-7461.

Bony, S., Stevens, B., Frierson, D. M. W., Jakob, C., Kageyama, M., Pincus, R., ... Webb, M. J. (2015). Clouds, circulation and climate sensitivity. *Nature Geosci.*, *8*, 261–268.

Byrne, M. P., Pendergrass, A. G., Rapp, A. D., & Wodzicki, K. R. (2018). Response of the intertropical convergence zone to climate change: Location, width, and strength. *Current Climate Change Reports*, *4*(4), 355–370. doi: 10.1007/s40641-018-0110-5

Byrne, M. P., & Schneider, T. (2016a). Energetic constraints on the width of the intertropical convergence zone. *J. Climate*, *29*, 4709–4721.

Byrne, M. P., & Schneider, T. (2016b). Narrowing of the itcz in a warming climate: Physical mechanisms. *Geophysical Research Letters*, *43*(21), 11–350.

Chen, J., Dai, A., & Zhang, Y. (2019). Projected changes in daily variability and seasonal cycle of near-surface air temperature over the globe during the twenty-first century. *Journal of Climate*, *32*(24), 8537–8561.

D'Agostino, R., Scambiati, A. L., Jungclaus, J., & Lionello, P. (2020). Poleward shift of northern subtropics in winter: Time of emergence of zonal versus regional signals. *Geophysical Research Letters*, *47*(19), e2020GL089325.

Donohoe, A., Atwood, A. R., & Byrne, M. P. (2019). Controls on the width of tropical precipitation and its contraction under global warming. *Geophysical Research Letters*, *46*(16), 9958–9967.

Donohoe, A., & Battisti, D. S. (2013). The seasonal cycle of atmospheric heating and temperature. *J. Climate*, *26*, 4962–4980.

Dwyer, J. G., Biasutti, M., & Sobel, A. H. (2012). Projected changes in the seasonal cycle of surface temperature. *Journal of Climate*, *25*(18), 6359–6374.

Eyring, V., Bony, S., Meehl, G. A., Senior, C. A., Stevens, B., Stouffer, R. J., & Taylor, K. E. (2016). Overview of the coupled model intercomparison project phase 6 (cmip6) experimental design and organization. *Geoscientific Model Development*, *9*(5), 1937–1958.

Feng, S., & Fu, Q. (2013). Expansion of global drylands under a warming climate. *Atmospheric Chemistry and Physics*, *13*(19), 10081–10094.

Geerts, B. (2003). Empirical estimation of the monthly-mean daily temperature range. *Theoretical and Applied Climatology*, *74*(3), 145–165.

Gelaro, R., McCarty, W., Suárez, M. J., Todling, R., Molod, A., Takacs, L., … others (2017). The modern-era retrospective analysis for research and applications, version 2 (merra-2). *Journal of climate*, *30*(14), 5419–5454.

Grise, K. M., Davis, S. M., Staten, P. W., & Adam, O. (2018). Regional and seasonal characteristics of the recent expansion of the tropics. *Journal of Climate*, *31*(17), 6839–6856.

Grünzweig, J. M., De Boeck, H. J., Rey, A., Santos, M. J., Adam, O., Bahn, M., … others (2022). Dryland mechanisms could widely control ecosystem functioning in a drier and warmer world. *Nature Ecology & Evolution*, 1–13.

He, J., & Soden, B. J. (2017). A re-examination of the projected subtropical precipitation decline. *Nature Climate Change*, *7*(1), 53–57.

Hersbach, H., Bell, B., Berrisford, P., Hirahara, S., Horányi, A., Muñoz-Sabater, J., … others (2020). The era5 global reanalysis. *Quarterly Journal of the Royal Meteorological Society*, *146*(730), 1999–2049.

Holmes, C. R., Woollings, T., Hawkins, E., & De Vries, H. (2016). Robust future changes in temperature variability under greenhouse gas forcing and the relationship with thermal advection. *Journal of Climate*, *29*(6), 2221–2236.

Huang, J., Li, Y., Fu, C., Chen, F., Fu, Q., Dai, A., … others (2017). Dryland climate change: Recent progress and challenges. *Reviews of Geophysics*, *55*(3), 719–778.

Lau, W. K., & Kim, K.-M. (2015). Robust hadley circulation changes and increasing global dryness due to co2 warming from cmip5 model projections. *Proceedings of the National Academy of Sciences*, *112*(12), 3630–3635.

Lu, J., Vecchi, G. A., & Reichler, T. (2007). Expansion of the Hadley cell under global warming. *Geophys. Res. Lett.*, *34*, L06805. (doi:10.1029/2006GL028443)

Manabe, S., Ploshay, J., & Lau, N.-C. (2011). Seasonal variation of surface temperature change during the last several decades. *Journal of climate*, *24*(15), 3817–3821.

Nguyen, H., Evans, A., Lucas, C., Smith, I., & Timbal, B. (2013). The Hadley circulation in reanalyses: Climatology, variability, and change. *J. Climate*, *26*, 3357–3376.

Nguyen, H., Hendon, H., Lim, E.-P., Boschat, G., Maloney, E., & Timbal, B. (2018). Variability of the extent of the hadley circulation in the southern hemisphere: a regional perspective. *Climate Dynamics*, *50*(1), 129–142.

Paffen, K. (1967). Das verhältnis der Tages-zur jahreszeitlichen Temperaturschwankung: Erläuterungen zu einer neuen Weltkarte als Beitrag zur allgemeinen Klimageographie (the relationship of diurnal to annual temperature variations). *Erdkunde*, *XXI*, 94–111.

Palmer, T., & Stevens, B. (2019). The scientific challenge of understanding and estimating climate change. *Proceedings of the National Academy of Sciences*, *116*(49), 24390–24395. doi: 10.1073/pnas.1906691116

Popp, M., & Lutsko, N. (2017). Quantifying the zonal-mean structure of tropical precipitation. *Geophysical Research Letters*, *44*(18), 9470–9478.

Riehl, H. (1954). *Tropical meteorology* (Tech. Rep.). McGraw-Hill.

Riehl, H., et al. (1979). *Climate and weather in the tropics.* Academic Press.

Ruane, A., Ranasinghe, R., Vautard, R., Arnell, N., Coppola, E., Cruz, F. A., … others (2021). Ipcc ar6 wgi chapter 12: Climate change information for regional impact and for risk assessment. In *Agu fall meeting abstracts* (Vol. 2021, pp. U13B–12).

Seidel, D. J., Fu, Q., Randel, W. J., & Reichler, T. J. (2008). Widening of the tropical belt in a changing climate. *Nature Geosci.*, *1*, 21–24.

Seviour, W. J., Davis, S. M., Grise, K. M., & Waugh, D. W. (2018). Large uncertainty in the relative rates of dynamical and hydrological tropical expansion. *Geophysical Research Letters*, *45*(2), 1106–1113.

Sobel, A. H., & Camargo, S. J. (2011). Projected future seasonal changes in tropical summer climate. *Journal of Climate*, *24*(2), 473–487.

Staten, P. W., Grise, K. M., Davis, S. M., Karnauskas, K., & Davis, N. (2019). Regional widening of tropical overturning: Forced change, natural variability, and recent trends. *Journal of Geophysical Research: Atmospheres*, *124*(12), 6104–6119.

Staten, P. W., Grise, K. M., Davis, S. M., Karnauskas, K. B., Waugh, D. W., Maycock, A. C., … Son, S.-W. (2020, 06). Tropical Widening: From Global Variations to Regional Impacts. *Bulletin of the American Meteorological Society*, *101*(6), E897-E904. doi: 10.1175/BAMS-D-19-0047.1

Staten, P. W., Lu, J., Grise, K. M., Davis, S. M., & Birner, T. (2018). Re-examining tropical expansion. *Nature Climate Change*, *8*(9), 768–775.

Stine, A. R., & Huybers, P. (2012). Changes in the seasonal cycle of temperature and atmospheric circulation. *Journal of Climate*, *25*(21), 7362–7380.

Stouffer, R., & Wetherald, R. (2007). Changes of variability in response to increasing greenhouse gases. part i: Temperature. *Journal of Climate*, *20*(21), 5455–5467.

Taylor, K. E., Stouffer, R. J., & Meehl, G. A. (2012). An overview of cmip5 and the experiment design. *Bulletin of the American meteorological Society*, *93*(4), 485–498.

Thorne, P., Donat, M., Dunn, R., Williams, C., Alexander, L., Caesar, J., … others (2016). Reassessing changes in diurnal temperature range: Intercomparison and evaluation of existing global data set estimates. *Journal of Geophysical Research: Atmospheres*, *121*(10), 5138–5158.

Thorne, P., Menne, M., Williams, C., Rennie, J., Lawrimore, J., Vose, R., … others (2016). Reassessing changes in diurnal temperature range: A new data set and characterization of data biases. *Journal of Geophysical Research: Atmospheres*, *121*(10), 5115–5137.

Troll, C. (1943). Thermische klimatypen der Erde (thermal climate types of Earth). *Petermanns Geogr. Mitteil.*, *43*(3/4), 81–89.

Wang, C., Zhang, L., Lee, S.-K., Wu, L., & Mechoso, C. R. (2014). A global perspective on cmip5 climate model biases. *Nature Climate Change*, *4*(3), 201–205.

Wang, K., & Clow, G. D. (2020). The diurnal temperature range in cmip6 models: Climatology, variability, and evolution. *Journal of Climate*, *33*(19), 8261–8279.

Waugh, D., Grise, K. M., Seviour, W., Davis, S., Davis, N., Adam, O., ... Simpson, I. R. (2018). Revisiting the relationship among metrics of tropical expansion. *J. Climate*.

Wild, M. (2009). Global dimming and brightening: A review. *Journal of Geophysical Research: Atmospheres*, *114*(D10).

Yang, G.-Y., & Slingo, J. (2001). The diurnal cycle in the tropics. *Monthly Weather Review*, *129*(4), 784–801.

Yettella, V., & England, M. R. (2018). The role of internal variability in twenty-first-century projections of the seasonal cycle of northern hemisphere surface temperature. *Journal of Geophysical Research: Atmospheres*, *123*(23), 13–149.

Yin, J., & Porporato, A. (2017). *Diurnal cloud cycle biases in climate models, nat. commun., 8, 2269.*

Supporting Information for ”Reduced tropical climate land area under global warming”

Ori Adam[1], Noga Liberty-Levi[1], Michael Byrne[2,3], Thomas Birner[4]

[1]The Fredy and Nadine Herrmann Institute of Earth Sciences, The Hebrew University, Jerusalem, Israel

[2]School of Earth and Environmental Sciences, University of St Andrews, St Andrews, UK

[3]Department of Physics, University of Oxford, Oxford, UK

[4]Meteorologisches Institut, Ludwig-Maximilians-Universität, Munich, Germany

Supporting figures and tables

1. Figure S1: Daily climatologies of $\Delta_{Seasonal}$ and $\Delta_{Diurnal}$
2. Figure S2: $\Delta_{Seasonal}$ and $\Delta_{Diurnal}$ in CMIP5 and CMIP6 models
3. Figure S3: PDFs of end of 20th and end of 21st centuries
4. Figure S4: PDFs of regional changes in tropical land areas
5. Figure S5: Agreement across CMIP5/6 models by grid point
6. Table S1: CMIP5 and CMIP6 models’ names and affiliations

Supporting information

a. Seasonal and diurnal temperature variations

The observed climatologies of surface temperature deviations from annual mean and of the diurnal surface temperature range are shown in Figure S1, zonally averaged over land. These variations are larger by factors of about 2 and 10 compared to the variations over oceans. However, the above factors can vary, as diurnal and seasonal land surface variations modulate adjacent ocean variations in some regions (Yang & Slingo, 2001).

If seasonal tropical temperature variations were determined solely by the seasonal march of peak insolation, temperatures near the equator would show two equinoctial peaks. The lack of a dominant semi-annual mode in temperature variations near the equator (Figure S1a) therefore indicates that additional processes, related to the dynamics of the tropical rain belt, are important (Riehl, 1954). The seasonal migrations of the tropical rain belt also affect diurnal temperature variations, which are smaller in heavily precipitating areas. Therefore, since we calculate $\Delta_{Diurnal}$ using annual means (derived from monthly means), we note that this definition fails to capture: (i) seasonal migrations of the equatorial minimum in $\Delta_{Diurnal}$, and (ii) increased $\Delta_{Diurnal}$ in subtropical latitudes ($\sim$20°) during winter.

b. Differences between CMIP5 and CMIP6 models

Figure S2 shows $\Delta_{Seasonal}$ and $\Delta_{Diurnal}$ in CMIP5 (pink) and CMIP6 (blue) models, averaged over land. The differences between the two CMIP phases the statistically insignificant in all tropical latitudes. We therefore analyze the two phases jointly.

c. Changes in tropical land area

Figure S3a,b compares end of 20th and end of 21st centuries' probability distribution functions (PDFs) of tropical land width (mean latitudinal extent of land where $\Delta_{Diurnal} > \Delta_{Seasonal}$) and of tropical land area (net land area where $\Delta_{Diurnal} > \Delta_{Seasonal}$), across the 45 CMIP5/6 models. A clear shift toward reduced tropical width and area is seen by the end of the 21st century, indicating a reduced net tropical extent under global warming (ensemble mean decrease in width and area is $2.9°$ and $3.1{\cdot}10^6$ km^2). Similar PDFs of the extent of the subtropical dry zones (SDZs), and of the width of the tropical rain belt (TRB), averaged globally and over land, are shown in Figure S3c-e.

Figure S4 shows regional PDFs of changes in tropical land area. Significant decrease is seen in the African and American sectors, whereas a negligible change is seen in the Asia–Western-Pacific sector. As an indication of the robustness of the projected changes, Figure S5a shows the sum over the sign of the change in $\Delta_{Diurnal} - \Delta_{Seasonal}$ across models, by grid point. The changes are most robust in the African and south American regions. Figure S5b-c shows similar sums due to the individual changes in $\Delta_{Seasonal}$ and $\Delta_{Diurnal}$ (i.e., holding $\Delta_{Diurnal}$ fixed in Figure S5b and holding $\Delta_{Seasonal}$ fixed in Figure S5c). The projected reduction in net tropical land area is thus primarily driven by increased $\Delta_{Seasonal}$ over Africa and the Americas, with some contribution by reduced $\Delta_{Diurnal}$ over northern Africa.

References

Bell, B., Hersbach, H., Simmons, A., Berrisford, P., Dahlgren, P., Horányi, A., ... others (2021). The era5 global reanalysis: Preliminary extension to 1950. *Quarterly Journal of the Royal Meteorological Society*, *147*(741), 4186–4227.

Hersbach, H., Bell, B., Berrisford, P., Hirahara, S., Horányi, A., Muñoz-Sabater, J., ... others (2020). The era5 global reanalysis. *Quarterly Journal of the Royal Meteorological Society*, *146*(730), 1999–2049.

Riehl, H. (1954). *Tropical meteorology* (Tech. Rep.). McGraw-Hill.

Yang, G.-Y., & Slingo, J. (2001). The diurnal cycle in the tropics. *Monthly Weather Review*, *129*(4), 784–801.

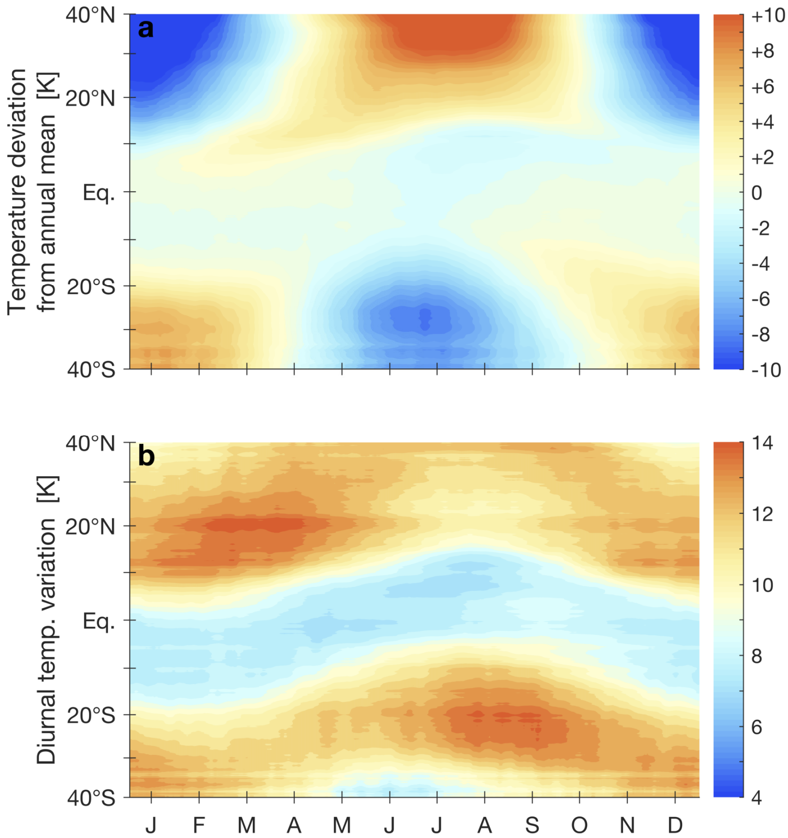

Figure S1. Daily climatologies of (**a**) surface temperature deviation from annual mean, and (**b**) diurnal surface temperature variations, zonally averaged over land areas. Data taken from ERA5 (Hersbach et al., 2020; Bell et al., 2021) for the years 1979–2019, smoothed with a 7-day centered running mean.

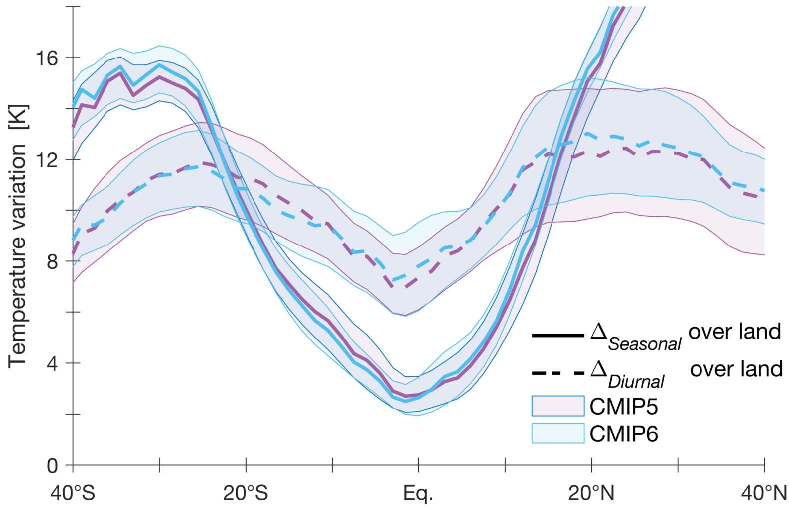

Figure S2. Amplitude of seasonal (solid) and diurnal (dashed) temperature variations ($\Delta_{Seasonal}$ and $\Delta_{Diurnal}$, respectively), zonally averaged over land areas, for CMIP5 (pink) and CMIP6 (blue) models. Bold lines show ensemble means; shading indicates ± 1 standard deviation across models in each CMIP phase.

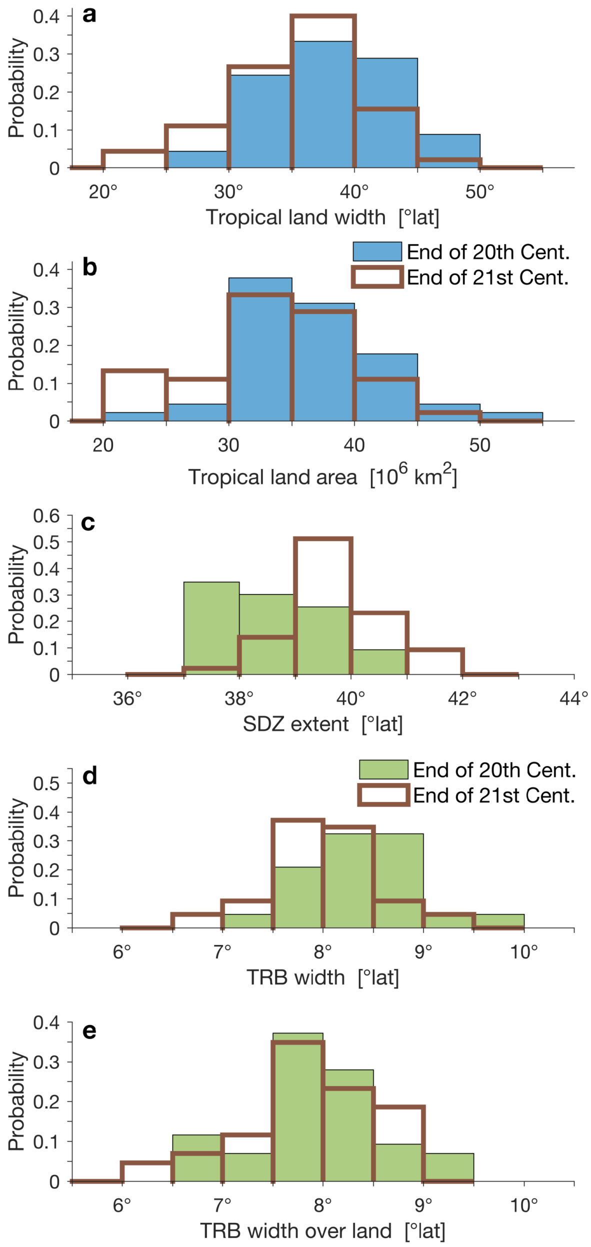

Figure S3. Probability distribution functions of (**a**) tropical land width (mean latitudinal extent of land where $\Delta_{Diurnal} > \Delta_{Seasonal}$), (**b**) tropical land area (net land area where $\Delta_{Diurnal} > \Delta_{Seasonal}$), (**c**) the extent of the subtropical dry zones (SDZs), (**d**) width of the tropical rain belt (TRB), and (**e**) width of the TRB over land. End of 20th century and end of 21st century values are shown in blue/green bars and brown lines, respectively. Note that the PDFs are composed of 45 models in panels a and b, and of 43 models in panels c–e.

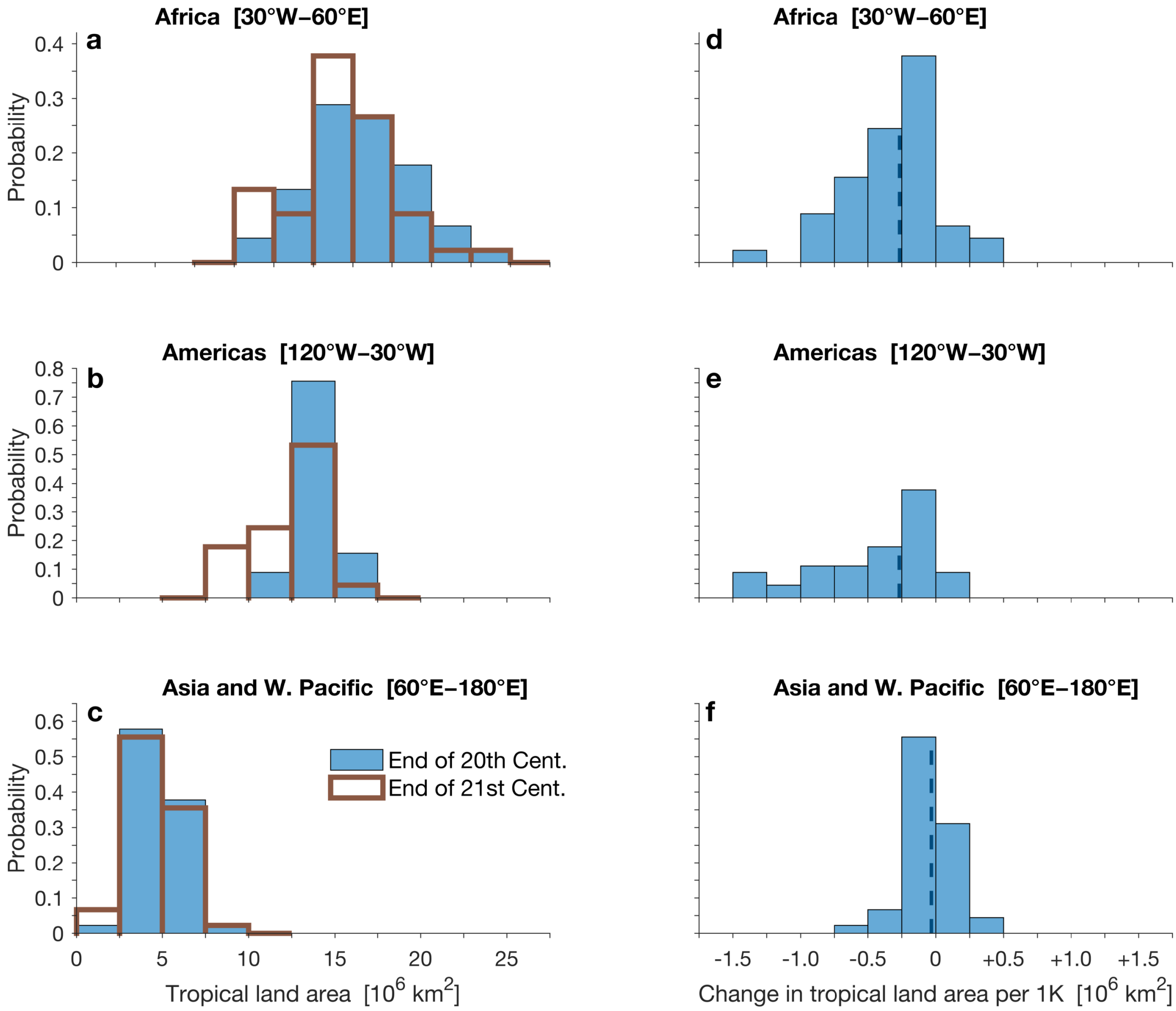

Figure S4. Left panels show the probability distribution functions (PDFs) of changes in tropical land area over the (**a**) African, (**b**) the Americas, and (**c**) Asia and western-Pacific sectors. Blue bars and brown lines indicate PDFs for the end of the 20th century (1980–1999) and end of 21st century (2080–2099), respectively. Right panels show PDFs of the corresponding changes, with vertical lines indicating medians.

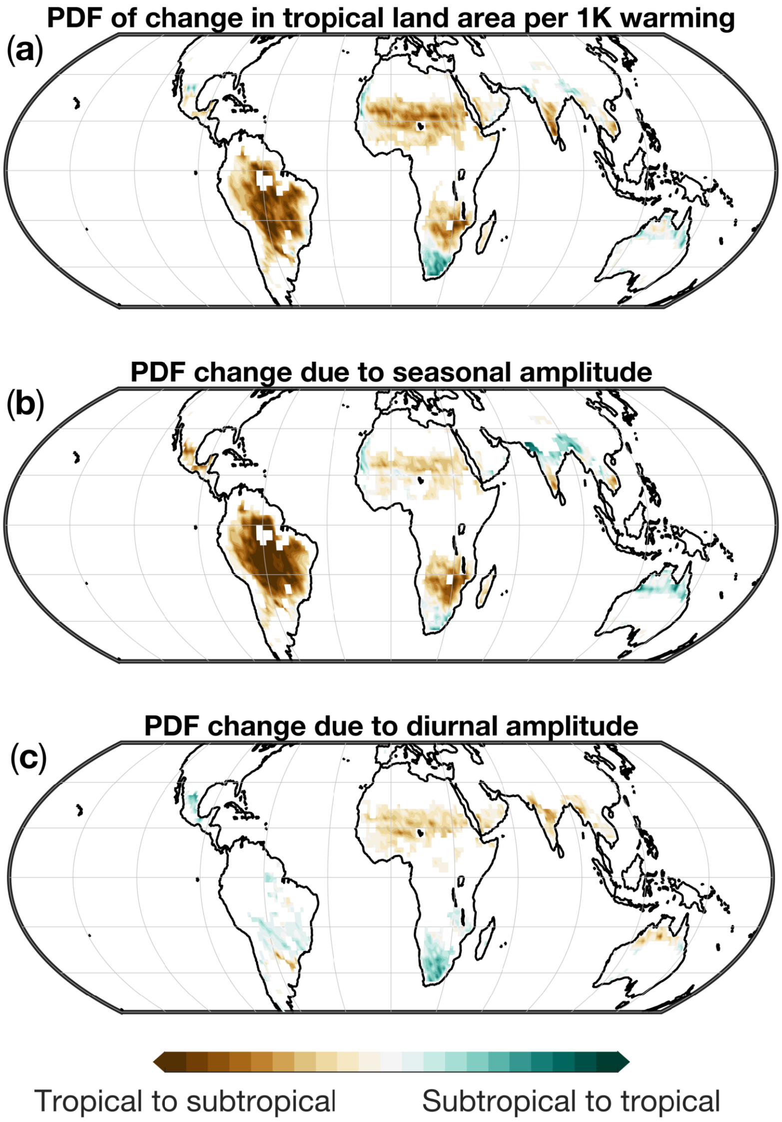

Figure S5. Sum over the sign of the change in $\Delta_{Diurnal} - \Delta_{Seasonal}$ across models by grid point, for (**a**) $\Delta_{Diurnal} - \Delta_{Seasonal}$, (**b**) changes due to $\Delta_{Seasonal}$ (i.e., $\Delta_{Diurnal}$ is held fixed), and (**c**) changes due to $\Delta_{Diurnal}$ (i.e., $\Delta_{Seasonal}$ is held fixed). Negative (brown) and positive (green) values indicate decrease and increase in tropical land area, respectively. White colors indicate equal number of models showing positive and negative changes in $\Delta_{Diurnal} - \Delta_{Seasonal}$.

Table S1. CMIP5 and CMIP6 models' names and affiliations. The two CMIP6 models for which precipitation minus evaporation is not available are marked with an asterisk.

Affiliation	**CMIP5 Model**	**CMIP6 Model**
CSIRO, and Bureau of Meteorology, Australia	ACCESS1-0	ACCESS-CM2
	ACCESS1-3	ACCESS-ESM1-5
	CSIRO-Mk3-6-0	
Beijing Climate Center (BCC), China		BCC-CSM2-MR
Chinese Academy of Science (CAS), China		CAS-ESM2-0*
Centro Euro-Mediterraneo sui Cambiamenti Climatici (CMCC), Italy	CMCC-CESM	CMCC-ESM2
	CMCC-CM	
	CMCC-CMS	
CCCma, Canada	CanESM2	CanESM5
CNRM and CERFACS, France	CNRM-CM5	
EC-Earth consortium		EC-Earth3
		EC-Earth3-veg
LASG/IAP, China		FGOALS-g3
FIO, QNLM, China		FIO-ESM-2-0
NOAA GFDL, USA	GFDL-CM3	GFDL-ESM4*
	GFDL-ESM2G	
	GFDL-ESM2M	
NASA / GISS, USA	GISS-E2-H	
	GISS-E2-H-CC	
	GISS-E2-R	
	GISS-E2-R-CC	
Met Office Hadley Centre, UK	HadGEM2-AO	
	HadGEM2-CC	
	HadGEM2-ES	
INM, Russia	inmcm4	INM-CM4-8
		INM-CM5-0
Institut Pierre Simon Laplace (IPSL), France		IPSL-CM6A-LR
JAMSTEC, AORI, and NIES, Japan	MIROC-ESM	MIROC6
	MIROC-ESM-CHEM	
	MIROC5	
Max Planck Institute for Meteorology (MPI), Germany	MPI-ESM-LR	MPI-ESM1-2-HR
	MPI-ESM-MR	MPI-ESM1-2-HR
Meteorological Research Institute (MRI), Japan	MRI-CGCM3	MRI-ESM2-0
	MRI-ESM1	
Norwegian Climate Centre, Norway	NorESM1-M	